Capturing Photons More Efficiently

Heinrich R. Schelbert

UCLA School of Medicine, Los Angeles, California

Among the scientific accomplishments recorded in *The Journal of Nuclear Medicine* is Hal Anger's groundbreaking contribution entitled, "Scintillation Camera with Multichannel Collimators" (*1*). In this article, Anger moves beyond the concept of pinhole imaging to an emerging, multiple–parallel-hole, concept for projecting photons onto an imaging screen because, in his words, "…for large gamma-ray emitting subjects, such as the brain or liver, collimators with large numbers of parallel holes…give the best combination of sensitivity and resolution." This forward-looking move to a new and more efficient approach to collimating photons profoundly impacted the emerging field of radionuclide imaging; it expedited and, importantly, expanded the potential of nuclear medicine imaging for new clinical applications and likely accelerated the growth of the emerging field of nuclear medicine. Imaging the uptake and distribution of radionuclides in organs for therapeutic purposes had begun only about 15 years before Anger's 1964 publication on parallel-hole collimators, when Benedict Cassen, a physicist at the UCLA Atomic Energy Project, demonstrated that nuclear imaging was not only feasible but also relevant for treating thyroid disease with radioiodine (*2*,*3*). Cassen's rectilinear scanner—which, in his early studies, consisted of a motorized collimated crystal-based radiation detector that moved back and forth over a radionuclidecontaining target organ such as the thyroid gland—produced an image readout or scan of an array of lines with dots of different intensities or densities, which was printed on paper or radiographic films. Envisioning a different concept of radionuclide imaging in which the entire organ could be imaged at once, Hal Anger, an electrical engineer at the Donner Laboratory at the University of California in Berkeley, pursued an approach in which photons originating from the thyroid gland pass through a pinhole and are projected onto an imaging screen. This screen consisted at first of photographic paper but was subsequently replaced by an initially 4-in-wide and later 11-in-wide sodium iodide scintillation detector crystal that Anger had coupled to a set of densely packed photomultiplier tubes (*4*–*6*).

Received May 1, 2020; revision accepted May 7, 2020.
For correspondence or reprints contact: Heinrich R. Schelbert, UCLA School of Medicine, B2-096 CHS, Mail Stop 956948, Los Angeles, CA 90095.
E-mail: hschelbert@mednet.ucla.edu

DOI: 10.2967/jnumed.120.248815

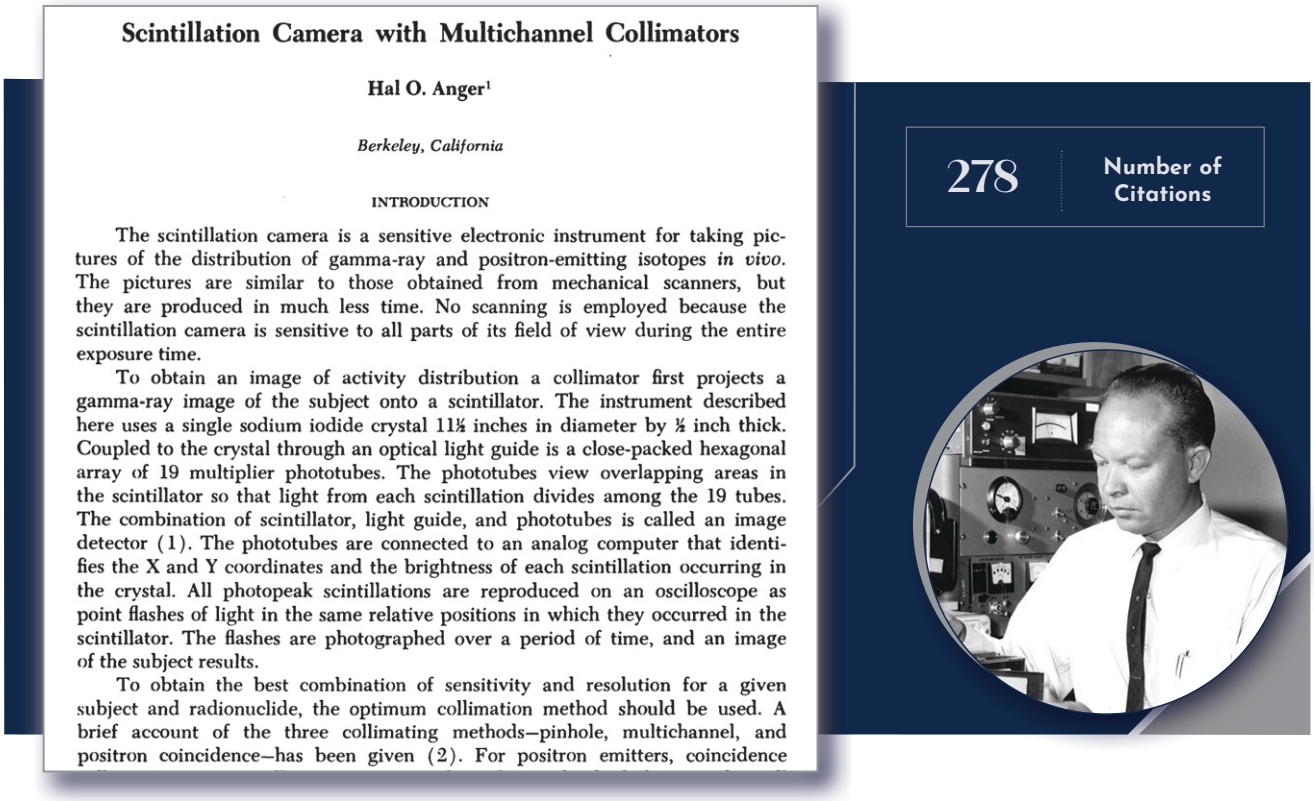

Scintillation Camera with Multichannel Collimators

Hal O. Anger[1]

Berkeley, California

INTRODUCTION

The scintillation camera is a sensitive electronic instrument for taking pictures of the distribution of gamma-ray and positron-emitting isotopes *in vivo*. The pictures are similar to those obtained from mechanical scanners, but they are produced in much less time. No scanning is employed because the scintillation camera is sensitive to all parts of its field of view during the entire exposure time.

To obtain an image of activity distribution a collimator first projects a gamma-ray image of the subject onto a scintillator. The instrument described here uses a single sodium iodide crystal 11½ inches in diameter by ¼ inch thick. Coupled to the crystal through an optical light guide is a close-packed hexagonal array of 19 multiplier phototubes. The phototubes view overlapping areas in the scintillator so that light from each scintillation divides among the 19 tubes. The combination of scintillator, light guide, and phototubes is called an image detector (1). The phototubes are connected to an analog computer that identifies the X and Y coordinates and the brightness of each scintillation occurring in the crystal. All photopeak scintillations are reproduced on an oscilloscope as point flashes of light in the same relative positions in which they occurred in the scintillator. The flashes are photographed over a period of time, and an image of the subject results.

To obtain the best combination of sensitivity and resolution for a given subject and radionuclide, the optimum collimation method should be used. A brief account of the three collimating methods—pinhole, multichannel, and positron coincidence—has been given (2). For positron emitters, coincidence

From the signal output of the set of photomultiplier tubes, and with an analog computer, Anger succeeded in using a novel centroiding technique to accurately localize where on the detector crystal the scintillation or light flash had occurred (*7*). Anger's invention of this centroiding technique, known today as Anger logic, proved to be the key for g-camera imaging and continues to be used in modern radionuclide imaging systems.

Anger's 1964 publication in *The Journal of Nuclear Medicine* is a testimony to his impressive analytic mind (*1*). He emphasizes distinct advantages of parallel-hole collimators, such as the "one-to-one size relationship between the subject and the image produced in the scintillator," the fact that the image "size is independent of the distance between the subject and the collimator," and the "uniform 'depth response'." Importantly, as Anger states, "the best combination of sensitivity and resolution for a given subject and radionuclide" can be achieved only through an optimal method of photon collimation, an objective that motivated the research presented in this publication. Anger describes a variety of collimator designs, carefully explores the performance properties of individual collimator components (e.g., the number, diameter, and shapes of collimator holes; the density of packing holes; and the thickness of septa), and derives formulas for a series of radionuclide-specific collimator designs of optimal sensitivity and spatial resolution. The paper underscores the importance of different collimator designs for different types of medical imaging by showing images of the liver and kidneys, for example, as well sets of serially acquired dynamic images. As if to summarize his findings, he points out and predicts that the "resulting greater speed with which pictures can be taken is a decided advantage in clinical situations. Several different views can be taken if desired, and the examination can still be completed in a relatively short time." An interesting sideswipe at Cassen's rectilinear scanner (still widely used at the time) can be seen in Anger's comment that even when used with high-energy photons, the overall sensitivity of his scintillation camera is "still considerably higher than that of focused-collimator mechanical scanners."

Looking back at the tremendous impact of Anger's work on nuclear medicine imaging, it is not surprising that the paper received more citations than any other publication in *The Journal of Nuclear Medicine* in the 1960s. The author had indeed correctly foreseen the lasting impact of Anger logic and parallel-hole collimation on state-of-the-art radionuclide imaging devices, including whole-body imaging systems and tomographic imaging with SPECT.

DISCLOSURE

No potential conflict of interest relevant to this article was reported.

ACKNOWLEDGMENTS

I thank Susan Nath for her editorial assistance in preparing this commentary.

REFERENCES

1. Anger HO. Scintillation camera with multichannel collimators. *J Nucl Med*. 1964; 5:515–531.
2. Bauer FK, Barrett TF, Cassen BC. Scintigrams of the thyroid gland: the diagnosis of morphologic abnormalities with I131. *Calif Med*. 1952;77:380–382.
3. Cassen B. Radioisotope scanning instrumentation. *Int Rec Med Gen Pract Clin*. 1957;170:139–143.
4. Anger HO. Use of a gamma-ray pinhole camera for in vivo studies. *Nature*. 1952;170:200–201.
5. Tapscott E. Nuclear medicine pioneer: Hal O. Anger—first scintillation camera is foundation for modern imaging systems. *J Nucl Med*. 1998;39(3):15N, 19N, 26N–27N.
6. Wagner HN Jr. Hal Anger: nuclear medicine's quiet genius. *J Nucl Med*. 2003; 44(11):26N–28N, 34N.
7. Tapscott E. Nuclear medicine pioneer, Hal O. Anger, 1920–2005. *J Nucl Med Technol*. 2005;33:250–253.

Scintillation Camera with Multichannel Collimators

Hal O. Anger

Donner Laboratory of Medical Physics and Biophysics and Lawrence Radiation Laboratory, University of California, Berkeley, California

INTRODUCTION

The scintillation camera is a sensitive electronic instrument for taking pictures of the distribution of gamma-ray and positron-emitting isotopes *in vivo.* The pictures are similar to those obtained from mechanical scanners, but they are produced in much less time. No scanning is employed because the scintillation camera is sensitive to all parts of its field of view during the entire exposure time.

To obtain an image of activity distribution a collimator first projects a gamma-ray image of the subject onto a scintillator. The instrument described here uses a single sodium iodide crystal 11½ inches in diameter by ½ inch thick. Coupled to the crystal through an optical light guide is a close-packed hexagonal array of 19 multiplier phototubes. The phototubes view overlapping areas in the scintillator so that light from each scintillation divides among the 19 tubes. The combination of scintillator, light guide, and phototubes is called an image detector (*1*). The phototubes are connected to an analog computer that identifies the X and Y coordinates and the brightness of each scintillation occurring in the crystal. All photopeak scintillations are reproduced on an oscilloscope as point flashes of light in the same relative positions in which they occurred in the scintillator. The flashes are photographed over a period of time, and an image of the subject results.

To obtain the best combination of sensitivity and resolution for a given subject and radionuclide, the optimum collimation method should be used. A brief account of the three collimating methods—pinhole, multichannel, and positron coincidence—has been given (*2*). For positron emitters, coincidence collimation gives excellent sensitivity and resolution for both large and small subjects. For small subjects containing gamma-ray emitters, pinhole collimation is the method of choice. It is used to obtain high-resolution pictures of small subjects such as the thyroid gland.

However, for large gamma-ray emitting subjects, such as the brain or liver, collimators with large numbers of parallel holes (*2–9*) give the best combination of sensitivity and resolution. A drawing of this type of collimator is shown with the scintillation camera image detector in Figure 1.

Parallel-channel collimators have properties that are different from those of other collimators. One characteristic is the one-to-one size relationship between the subject and the image produced in the scintillator. In addition the size is independent of the distance between the subject and the collimator. This is an advantage in diagnostic situations where an organ lies at an unknown depth and its size is to be determined.

DOI: 10.2967/jnumed.120.248815A

Sharpest image resolution is obtained in the parts of the subject lying closest to the collimator. However, parallel-channel collimators can be designed to provide resolution equal to focused collimators in the deeper parts of the subject. The "depth of focus" of parallel-channel collimators can be much greater than that provided by focused collimators.

Parallel-channel collimators have substantially uniform "depth response," or in other words, equal sensitivity to activity at different depths in air. In tissue the depth response is of course modified by tissue attenuation.

Many combinations of hole diameter, length, and septal thickness are possible in multichannel collimators. Formulas are given in the next section to assist in designing collimators that have maximum efficiency for a given resolution and maximum gamma-ray energy. The collimators are most efficient when they can be designed for use with low-energy gamma rays, because the septa can be thinner and more holes can be packed into a given area. However, even when the collimators are designed for use with gamma rays of 0.4 MeV or more, the overall sensitivity of the scintillation camera is still considerably higher than that of focused-collimator mechanical scanners.

DESIGN OF PARALLEL-CHANNEL COLLIMATORS

Mathematical analysis of the image produced by a parallel-channel collimator is rather complex compared with pinhole collimation or positron coincidence collimation. In the latter two methods, a point source in the subject is imaged as a disc on the image detector. With multichannel collimators, gamma rays from a point source may strike the image detector in several areas, because they may travel through more than one of the holes to reach the scintillator. The shape of the irradiated areas depends on the shape of the holes, their distribution pattern, and the placement of the point source relative to the holes.

The mathematical analysis of this type of collimator is simplified if the assumption is made that the collimator moves sideways in the manner of a Bucky filter during the exposure time. Formulas have been derived that give the sensitivity and resolution as a function of hole diameter, length, and septal thickness. They have been derived by (a) assuming that the collimator moves relative to the subject and image detector during the entire exposure time, (b) determining the fraction of the time that a point source in the subject is visible to each element in the image detector and the solid angle of each element, and (c) integrating to determine the overall geometric efficiency.

For example, consider a collimator consisting of a rectangular array of square holes as shown in Figure 2. This section view shows a plane through the center of a row of holes. The width of the holes is d, the length is a, and the septal thickness is t. The distance from the radioactive subject to the near end of the

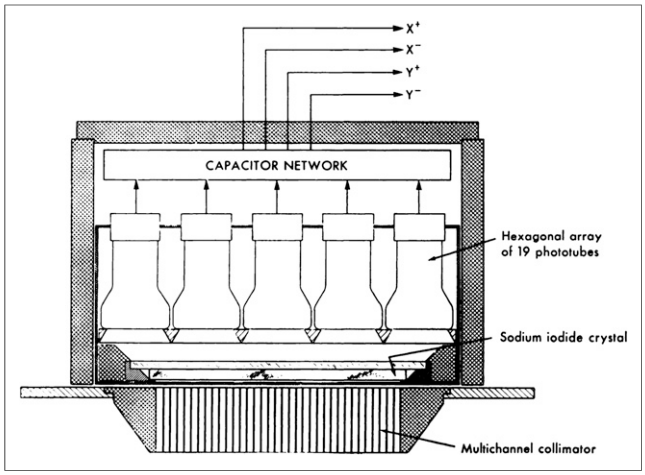

FIGURE 1. Scintillation camera image detector with multichannel collimator.

collimator is b, and the distance from the central plane of the scintillator to the other end of the collimator is c.

If the collimator is stationary, the distribution of gamma rays has the irregular shape shown at the top of Figure 2, but if the collimator moves in the direction shown, the average distribution of gamma rays that strike the scintillator has a triangular shape. The intensity is then a maximum at point o directly above the point source, and it falls linearly to zero, assuming opaque septa, at points q and q′. The distance oq, which is approximately equal to the full width of the gamma-ray intensity curve at half maximum, is defined as the geometric resolution-distance R.

From geometric considerations, it can be shown that

$$R = \frac{d(a+b+c)}{a}. \tag{1}$$

As expected, the resolution-distance R is smallest, or in other words the image is sharpest, when the distances b and c are small.

The geometric efficiency of the collimator is given by the formula

$$g = \left[\frac{Kd^2}{a(d+t)}\right]^2, \tag{2}$$

where g is defined as the number of gamma rays that pass through the channels divided by the total number emitted by the subject. Scattered gamma rays and any that travel through the septa are not included. It should be noted that g is independent of b, the distance between the subject and the collimator, providing the subject is completely imaged within the boundaries of the scintillator. Therefore the counting rate of a subject in air should be independent of the distance from the collimator to the subject. This has been found by experiment to be approximately true. The value of the constant K depends on the shape of the holes and their distribution pattern. It has been determined mathematically and confirmed approximately by experiment that K = 0.282 for square holes in a square array and K = 0.238 for round holes in a hexagonal array.

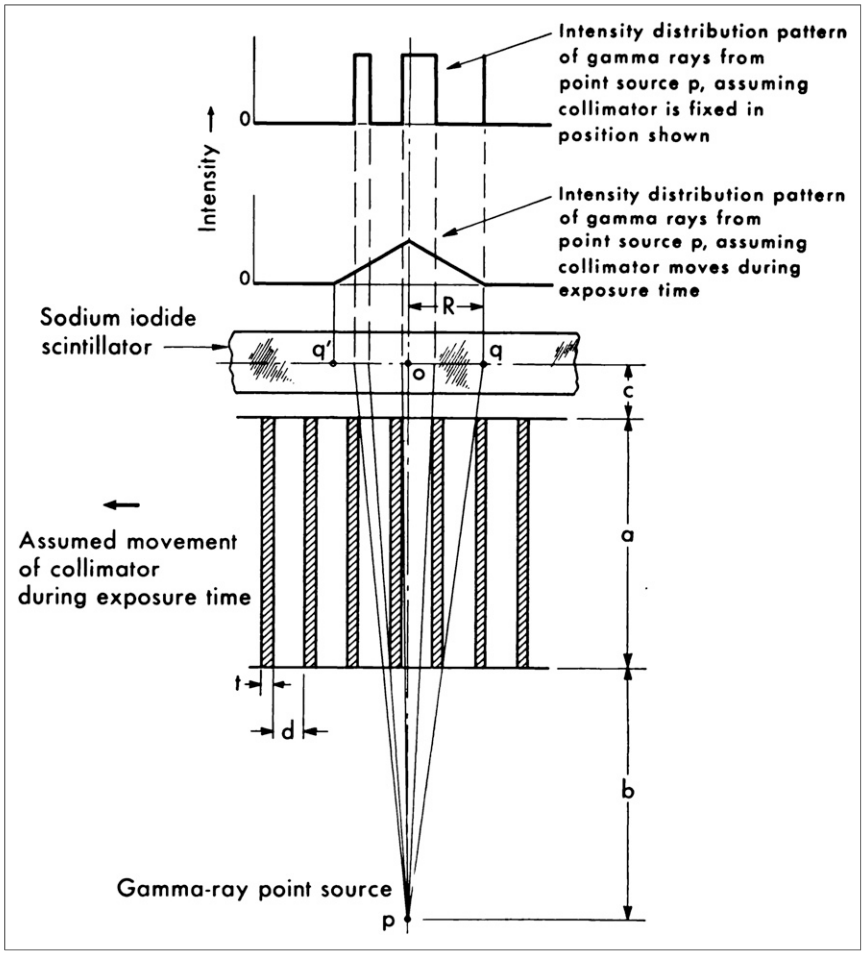

FIGURE 2. Section view of parallel-channel collimator showing gamma-ray pathways and irradiated areas of scintillator.

The shortest distance a gamma ray can travel through septal material when taking the unwanted path of minimum attenuation pr, shown in Figure 3, is w. From geometric considerations, w and t are approximately given by

$$w = \frac{at}{2d+t} \quad \text{or} \quad t = \frac{2dw}{a-w}. \tag{3}$$

From experimental studies, it has been determined that acceptable images result when the narrow-beam (Compton + photoelectric) attenuation of gamma rays taking the path pr is 95% or more. Assuming a given collimator material and gamma-ray energy, the distance w can be calculated. With w known, the minimum permissible septal thickness can be calculated for any hole diameter and length.

The sensitivity S in terms of dots per minute recorded on the picture per microcurie of activity in air is given by

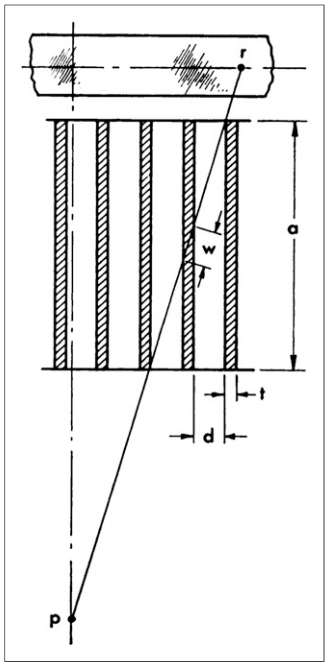

FIGURE 3. Path of minimum attenuation for gamma rays penetrating collimator septa.

$$S = 2.2 \times 10^6 \varepsilon f_a \frac{K^2 d^4}{a^2 (d+t)^2}, \quad (4)$$

where f_a is the abundance factor of the gamma ray, or the average number of gamma rays of a given energy emitted per disintegration. The photopeak counting efficiency ε is defined as the fraction of gamma rays incident on the scintillator that produce a dot on the picture when the pulse-height selector window is adjusted to accept nearly all the photopeak scintillations. Values of ε are given in other papers. (*1*,*2*,*10*). With the above equations, collimators can be designed that have optimum hole diameter, length, and septal thickness for a given subject-to-collimator distance, maximum gamma-ray energy, and desired resolution.

DEPTH OF FOCUS AND DEPTH RESPONSE

Since clinical subjects are nearly always several inches thick, the "depth of focus", or the depth over which a relatively sharp image is obtained, must be taken into account when evaluating any collimation method. The resolution of focused collimators is best for the parts of the subject at the geometric focus, which is usually 3 inches from the collimator. Their depth of focus is limited, and planes closer and farther away are less sharply resolved (*11*,*12*).

In comparison, the resolution of parallel-channel collimators is best for the parts of the subject closest to the collimator, and the resolution decreases with increasing distance. However, a parallel-channel collimator can be designed to give as good resolution as desired at any depth. For instance, it can be designed to have the same resolution at 3-inch distance as a focused collimator. Then it will have greater depth of focus because it will sharply resolve all the closer planes while the focused collimator will not.

Both collimating methods have "uniform depth response" in air, or equal counting sensitivity for activity at different depths. However, neither has uniform depth response in tissue because of gamma-ray scattering and absorption. It might be thought that because a stationary focused collimator has a maximum response to a point source on the axis at a distance of 3 inches (*13*), it would be more sensitive to activity lying on that plane in an actual scanning situation. This is not the case, as indicated by others (*12*,*14*,*15*) and confirmed experimentally by the author. Under working conditions, the "depth response" of the two collimating methods is the same, and each decreases with distance only because of tissue attenuation.

PARAMETERS OF TYPICAL COLLIMATORS

Parallel-channel collimators with hexagonal arrays of round holes can be made by (a) drilling holes in a plate, (b) cementing together lengths of tubing, or (c) casting the entire collimator in a suitable mold. Rectangular arrays of square holes have been made by (d) cementing together strips of lead or tungsten, (e) pressing sheet lead into W-shaped sections and cementing them together, and (f) cementing alternate strips of lead foil and balsa wood, cutting them crosswise into strips, and cementing these alternately with lead foil. This last technique is used to make low-energy collimators.

The parameters of eight typical collimators designed for maximum efficiency consistent with the stated geometric resolution

TABLE I

Parameters of Typical Parallel-Channel Collimators With Hexagonal Array of Round Holes. Collimator Material Is Lead and Scintillator Is 1/2-Inch-Thick Sodium Iodide. The Calculated Sensitivity is Given for Several Radionuclides. All Dimensions in Inches

Collimator	1	2	3	4	5	6	7	8	"A"
Resolution	Med.	High	Med.	High	Med.	High	Med.	High	High
Nominal maximum γ-ray energy	.20	.20	.28	.28	.36	.36	.41	.41	.36
Resolution-distance (R) at b = 1	.42	.28	.45	.30	.49	.32	.50	.34	.35
Resolution-distance (R) at b = 2	.57	.39	.60	.40	.62	.41	.63	.42	.43
Resolution-distance (R) at b = 3	.75	.50	.75	.50	.75	.50	.75	.50	.51
Resolution-distance (R) at b = 4	.92	.61	.90	.60	.88	.59	.87	.58	.59
Hole length (a)	1.0	1.0	1.5	1.5	2.2	2.2	2.6	2.6	3.0
Hole diameter (d)	0.167	0.111	0.225	0.150	0.290	0.193	0.320	0.213	0.237
Septum thickness (t)	.045	.030	.094	.063	0.133	.089	0.160	0.106	0.075
No. of holes in 11-inch dia. area	2480	5600	1090	2450	620	1400	490	1090	1165
Calculated sensitivity (Dots/min/μC of radionuclide in air)									
Ce^{139}	1280	570	860	380	610	270	500	220	270
Hg^{203}	—	—	410	180	290	130	240	105	130
I^{131}	—	—	—	—	180	78	145	65	78
Au^{198}	—	—	—	—	—	—	146	65	—

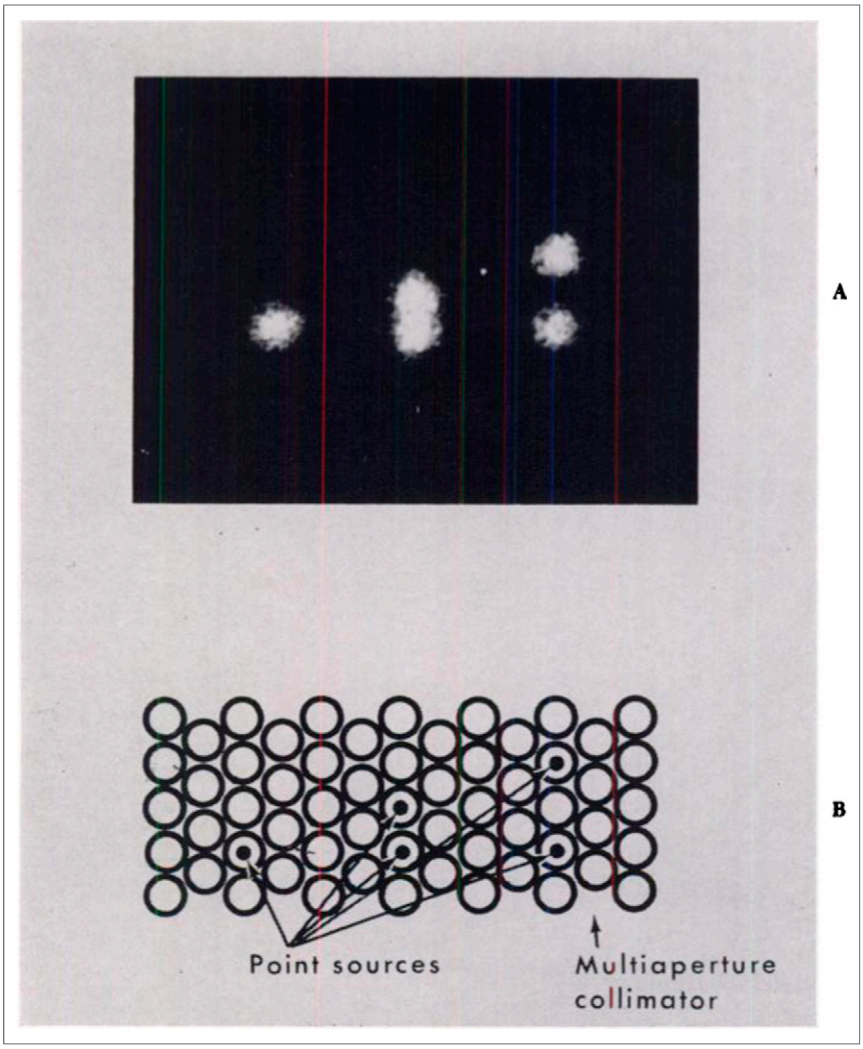

FIGURE 4. Enlarged section of image showing 5 point sources of Ba^{133} resolved by the "A" multichannel collimator. Sources are 1 inch from collimator and on the axes of holes shown in diagram.

and maximum gamma-ray energy are given in Table I. The material is lead, and all have hexagonal arrays of round holes.

The calculated overall sensitivity in terms of dots/minute/μc takes into account the abundance factors of the principle gamma rays. The contribution of the high-energy components of I^{131} was not included.

The parameters of a ninth collimator, designated as "A", are also included. This collimator was constructed before the formulas were derived, and has parameters that are slightly less than optimum, though its characteristics are similar to those of collimator No. 6. Collimator "A" has a nominal maximum gamma-ray energy of 0.36 MeV. It was used for all the liver, kidney, and thyroid-area examples that follow.

A collimator identical to No. 3 has also been constructed and tested in clinical use. It was designed for a maximum gamma-ray energy of 0.28 MeV and was used to take the brain pictures in the examples that follow. It was not used for the kidney pictures because collimator "A" has greater depth of focus and gives better results in this application. Collimator "A" was made by technique (b) above, and No. 3 was made by technique (a). Both have about 1,100 holes in an 11-inch diameter area.

A collimator designed for gamma rays less than 0.20 MeV has been made by technique (f) above. It has a rectangular array of 4000 square holes 0.11 inch wide by 1 inch long. In clinical use, it has produced pictures of brain tumors with exposures as short as 10 seconds when 2.5 Mc to Tc^{99m} was administered in the form of pertechnitate (*19*). Preliminary results obtained with this tracer compound will be presented in a later report (*20*).

Calculations indicate that higher sensitivity can be achieved if the collimators are made of tungsten alloy. The improvement results from having thinner septa and therefore more holes of the same diameter per unit area. The increase in sensitivity varies from 21 per cent for collimators designed for 0.28 MeV maximum to 30 per cent for those designed for 0.41 MeV.

PERFORMANCE OF COLLIMATORS

Since no material is completely opaque to gamma rays, the performance of the collimator is not exactly as predicted. The measured dots/minute/microcurie of radionuclide obtained from the existing collimators is larger than the calculated values at the higher gamma-ray energies. The increased count is caused by (a) gamma rays that travel through collimator material near the ends of the holes, (b) small-angle scattering of gamma rays by the channel walls, and (c) septal penetration. With some nuclides, part of the excess is caused by high energy components in the gamma-ray spectra that produce Compton events in the crystal.

When collimator "A" is used with I^{131}, about 85 per cent more than the theoretical number of counts are detected. Calculations indicate that about $^1/_3$ of the excess is due to reason (a) above. This calculation was made by assuming that the effective length of the collimator is equal to its geometric length less twice the mean free path of the gamma ray in the collimator material (*16*). Probably only a small amount of the excess is due to reason (b) (*16*). The rest is presumably due to (c). When Hg^{203} is used with the "A" collimator, the excess count is about 25 per cent, nearly all of which is caused by reason (a). Collimator No. 3 at its nominal maximum gamma-ray energy of 0.28 MeV gives an excess count of 35 per cent. Over $^3/_4$ of the excess in this case is calculated to be due to reason (a).

Although there is apparently a large amount of septal penetration at the higher gamma-ray energies, its effects are not normally visible in clinical pictures. The effect has been seen with the "A" collimator when small hot areas, such as the thyroid gland, are greatly overexposed. Then the "starfish" effect seen in focused collimators is visible (*17*).

Septal penetration can of course be reduced by making the collimators of tungsten alloy. Calculations indicate that for most collimators the number of gamma rays taking the path pr in Figure

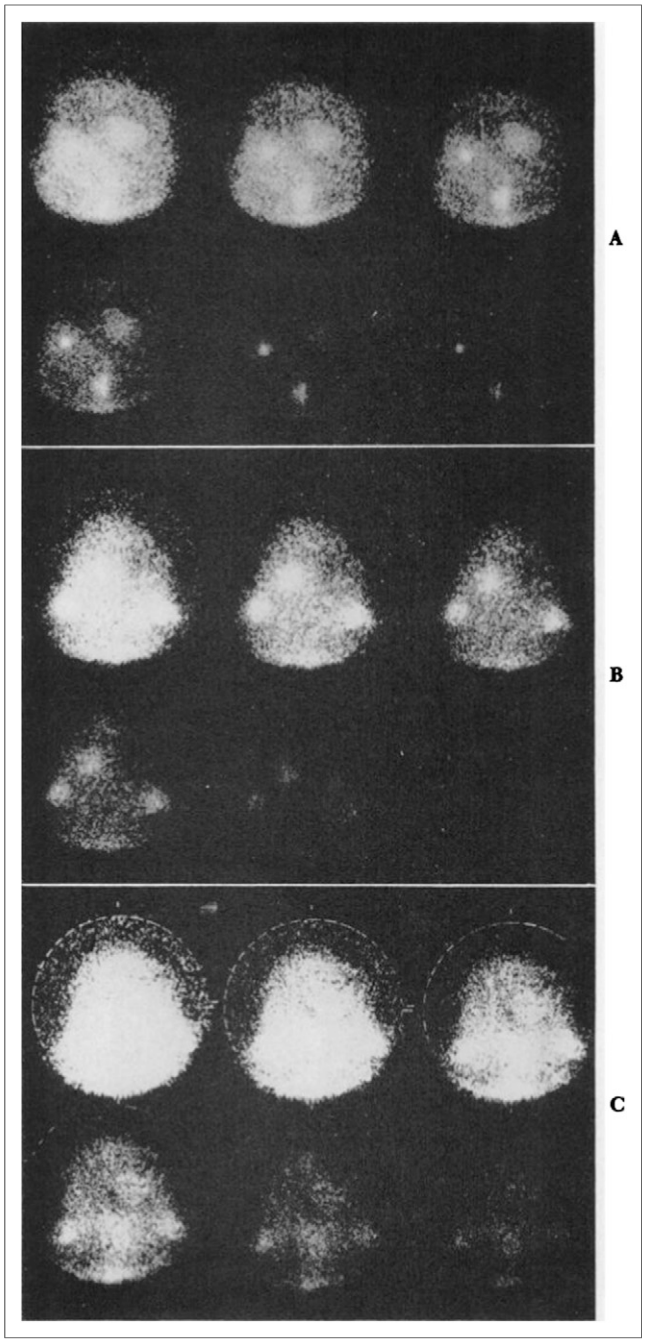

FIGURE 5. Pictures of brain lesion taken with Hg^{203} Neohydrin showing (A) left lateral view, (B) back view, and (C) frontal view. The six images of each view were obtained simultaneously in a 5-minute exposure. A prominent lesion and two marker sources are shown in each view, as well as an outline of the head due to body background.

3 would be $^1/_3$ as great with the denser material if the dimensions in Table I are not changed.

In the derivation of Eqs. (1) through (4), it was assumed that the collimator moved during the exposure time to provide a smooth distribution of gamma rays at the scintillator. This technique has not been used in taking pictures, however. The "collimator pattern" produced by stationary collimators is visible occasionally when small sources are imaged. With subjects larger than the thyroid gland, the effect has not been visible with the existing collimators.

Up to this point, only the theoretical geometric resolution of the collimator has been discussed. The overall resolution of the scintillation camera depends on the following factors: (a) the actual resolution of the gamma-ray image projected by the collimator, (b) the translation of this image into a light image by the scintillator, and (c) the reproduction of the scintillator image on the oscilloscope and the subsequent photographic image. The resolution lost in step (b) has been calculated to be very small for ½-inch-thick sodium iodide (*10*). Some resolution is lost in step (c), but the amount is not large for gamma rays with more than 0.15 MeV (*1*). The major factor that determines the overall resolution of the scintillation camera is the performance of the particular collimator used.

A demonstration of the overall resolution is shown in Figure 4A. Five point sources of Ba^{133} were placed 1 inch from the "A" collimator and on the axis of certain holes shown in Figure 4B. An enlargement of the central portion of the resulting picture shows the resolution obtained. Gamma rays traveling through adjacent holes produced adjacent white areas on the picture, while those separated by a blank hole in the collimator produced clearly separated spots.

CLINICAL PICTURES

The following examples of clinical pictures were taken with the scintillation camera and two of the parallel-channel collimators.

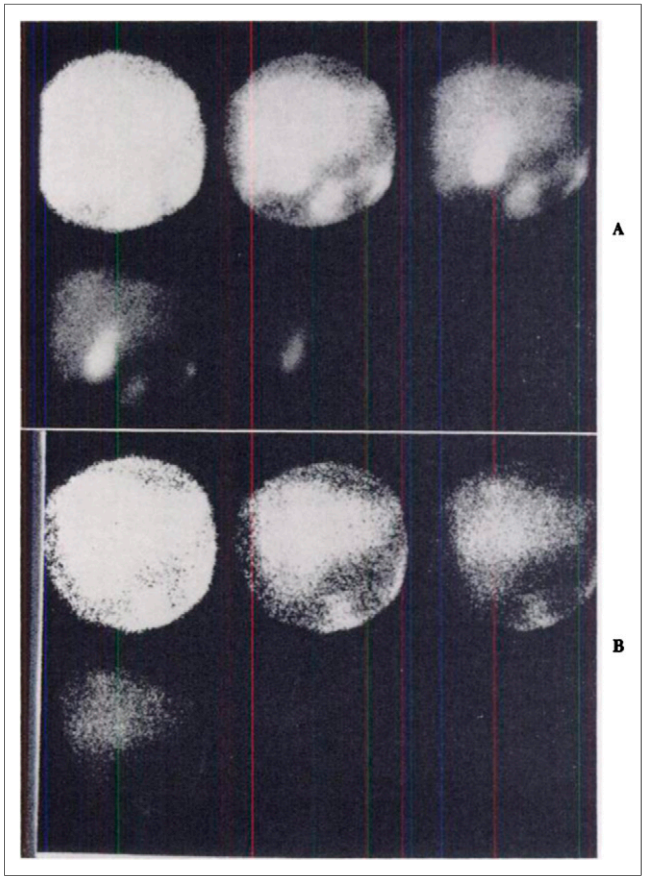

FIGURE 6. (A) Picture of adult liver taken after administration of 250 microcuries of I^{131} rose bengal. Exposure time was 10 minutes. (B) A 5-minute exposure of adult liver after administration of 200 microcuries of rose bengal. A defect is visible at upper left.

Three views of an adult patient with a brain lesion are shown in Figure 5. The pictures, showing (A) left lateral, (B) back and (C) frontal views, were taken 4 hours after the administration of 700 microcuries of Hg^{203} Neohydrin. The lesion is clearly visible in (A) and (B), and is less clearly visible in (C). The exposure time was 5 minutes with the No. 3 collimator for each of the three views. Marker sources of Ba^{133} were placed at the comer of the eye and the lower margin of the ear lobe in the lateral view, and at the ear canals in the frontal and back views. The six images with graded density were obtained simultaneously with a six-lens oscilloscope camera (*2*,*18*).

A picture of an apparently normal adult liver, taken with the "A" collimator, is shown in Figure 6A. It was taken 2 hours after the administration of 250 microcuries of I^{131} rose bengal. The exposure time was 10 minutes. The gall bladder is shown at the center, and bowel loops are shown at the lower right. In Figure 6B, the liver of another patient shows an apparent defect at the upper left. The exposure time in this example was 5 minutes, and the dose was 200 microcuries.

Multichannel collimators are used with the scintillation camera to take neck survey pictures of thyroid patients. The purpose is to show all active thyroid tissue within a 9- to 10-inch-diameter circle. Following the survey, a high resolution close-up picture of the thyroid gland is taken with a triple-aperture pinhole collimator (*2*). Pictures of the neck area of two patients, taken 24 hours after the ingestion of 50 microcuries of I^{131}, are shown in Figure 7A and B. The three graded-density images in each example were obtained with a three-lens oscilloscope camera. Exposure time was 5 minutes with the "A" collimator. A short extension of the upper part of the right lobe is visible in Figure 7A, but otherwise the pictures show that the area around the thyroid is clear of radioactive lymph nodes and substemal and thyroglossal extensions.

A 10-minute exposure of a thyroid phantom containing 5.9 microcuries of mock I^{131} is shown in Figure 7C. A suggestion of two cold nodules can be seen. These nodules are very clearly outlined in a 10-minute triple-aperture picture of the same phantom shown in an earlier publication (*2*).

Pictures of human kidneys taken with collimator "A" are shown in Figure 8. All these examples were taken from the back with the patient lying face down. The first two show a normal subject with an estimated 50 microcuries of Hg^{203} Neohydrin in the kidneys. The exposure times were 10 and 2 minutes respectively. Part of the liver appears to the right in each of the examples. The picture shown in Figure 8C was taken 20 minutes after the intravenous injection of 200 microcuries of I^{131} hippuran. In this 5-minute exposure, the hippuran is shown to be in the renal pelvis of both kidneys. The patient had bilateral kidney disease, resulting in a slow clearing time. The high body background is due to hippuran that had not been cleared from the blood. The two small spots between the kidneys are radioactive marker sources at the eleventh thoracic and second lumbar vertebrae.

Two sequences from a time-lapse motion picture of a patient with stenosis of the left renal artery are shown in Fig. 9A. Two hundred microcuries of I^{131} hippuran were given intravenously, and pictures were taken at the rate of two frames per minute with the "A" collimator. Though the degree of stenosis was mild, some delay in the filling of the left kidney is apparent, as well as a reduction in the peak uptake.

The time-lapse sequence in Figure 9B shows I^{131} rose bengal in the liver and intestine of a 3-month old girl. She had previous surgery for biliary atresia in which a fistula was created between the liver and duodenum. Later she had recurrent fever and jaundice, and it was thought the fistula may have closed. The time-lapse pictures show patency of the surgically created duct, since rose bengal is shown moving about in the intestine 1 hour after administration. The tracer dose was 50 microcuries, and pictures were taken at the rate of one frame every 2 minutes with the "A" collimator.

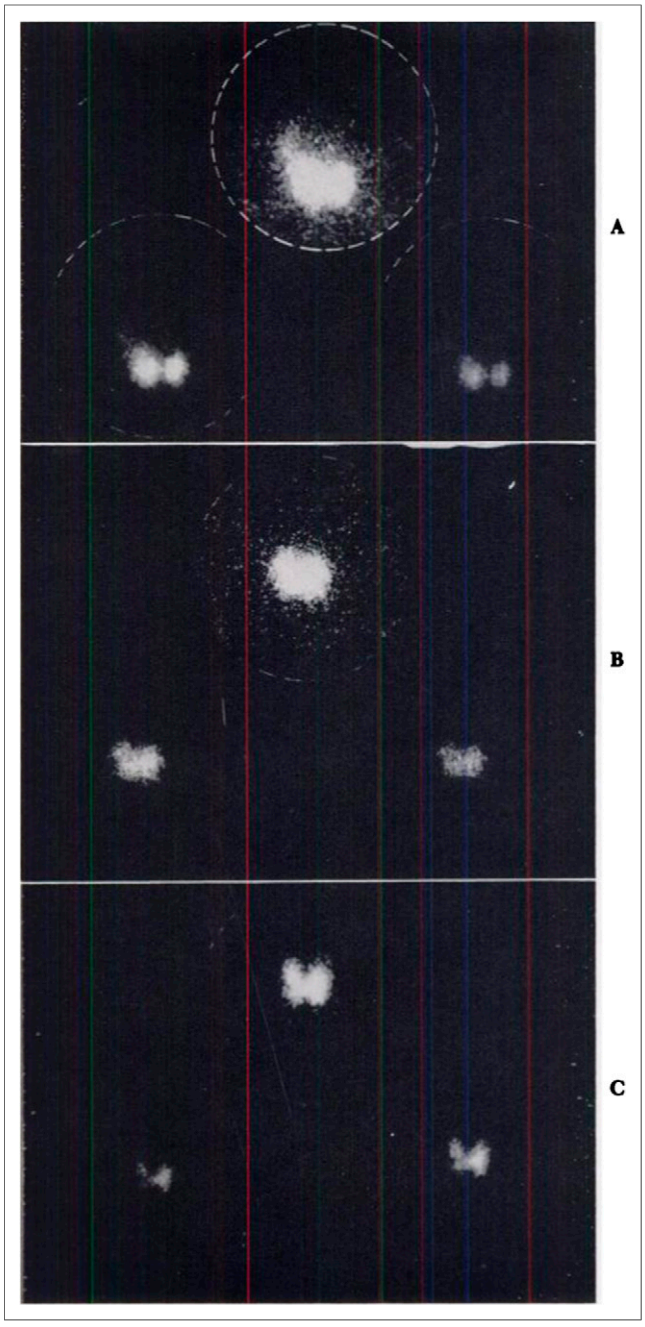

FIGURE 7. (A and B) Views of human thyroid and thyroid area. This type of survey shows any abnormal uptake of radioiodine in a 9-10 inch diameter area. The three images with graded density were obtained in a single 5-minute exposure. (C) Ten-minute exposure of thyroid phantom containing 5.9 microcuries of mock I^{131}.

CONCLUSION

The sensitivity of the scintillation camera when it is used with multichannel collimators is appreciably higher than focused-collimator

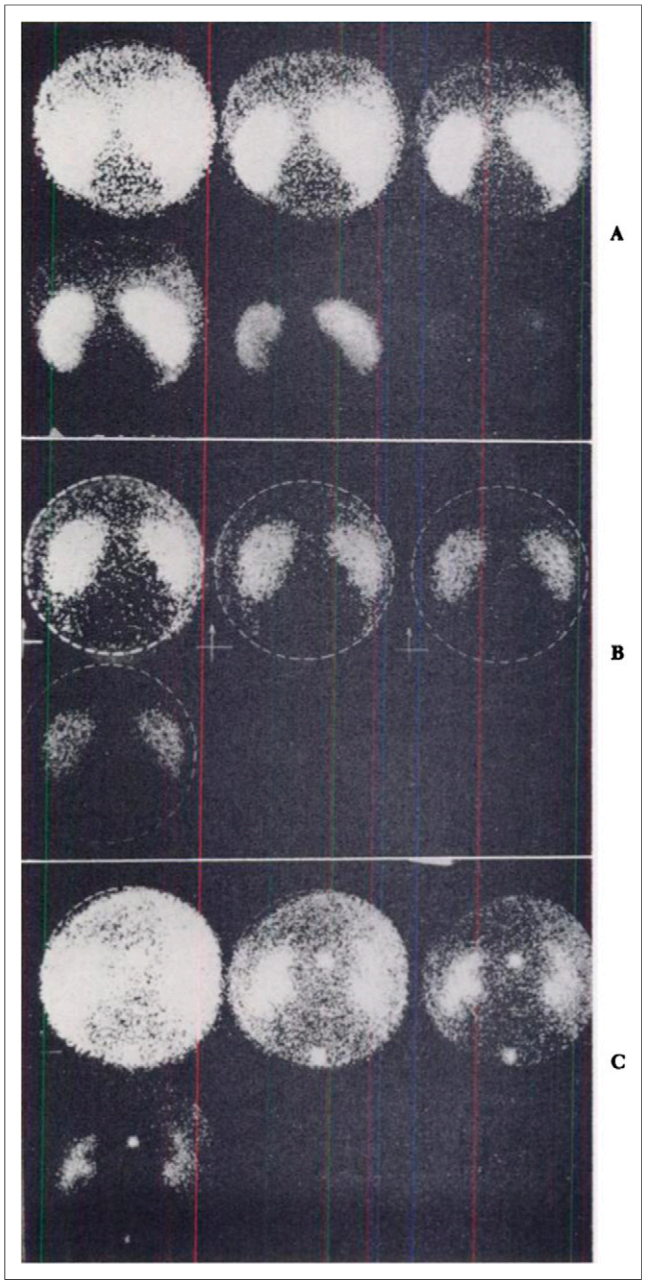

FIGURE 8. A and B Pictures of normal human kidneys taken with Hg^{203} Neohydrin. Exposure times were 10 and 2 minutes. (C) Renal pelvis of diseased kidney shown in a 5-minute exposure 20 minutes after adminstration of 200 microcuries of I^{131} hippuran.

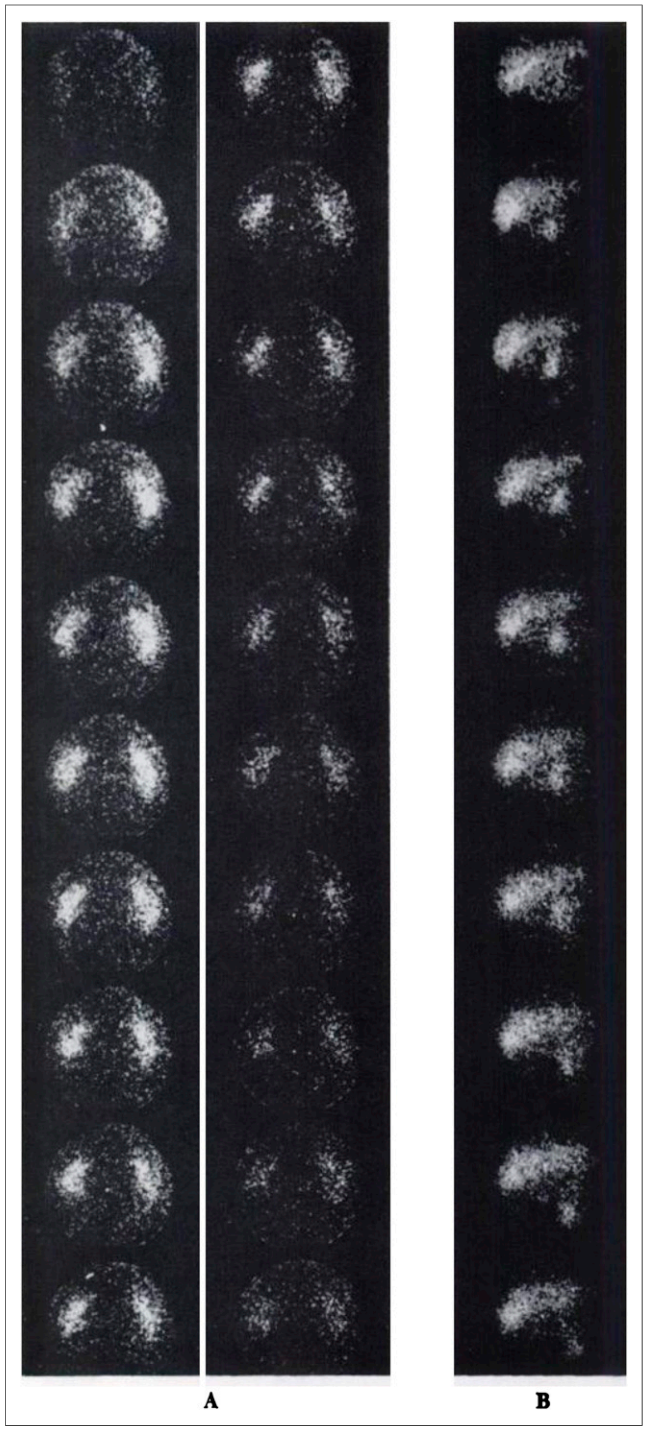

FIGURE 9. (A) Time lapse sequence showing I^{131} hippuran going through human kidneys. Exposure time was 30 seconds per picture. (B) Time lapse sequence showing excretion of I^{131} rose bengal from liver of girl. Exposure time was 2 minutes per picture (2).

mechanical scanners. The resulting greater speed with which pictures can be taken is a decided advantage in clinical situations. A number of different views can be taken if desired, and the examination can still be completed in a relatively short time. Alternatively, the amount of radioactive tracer can be reduced to minimize the radiation dose to the patient.

The scintillation camera has the further advantage that it is continuously sensitive to all parts of the subject within its field of view. Tracer compounds with short effective half-times can be used without the distortion inherent in scanners. Because of this and the high sensitivity, rapid sequences of still pictures or time-lapse movies can be taken to show the function of an organ.

ACKNOWLEDGMENTS

The author is indebted to Dr. John H. Lawrence for his support of this work. The assistance of Mr. Philip Yost is acknowledged. The clinical examples were obtained with the collaboration of Dr. Alexander Gottschalk, Dr. Howard G. Parker, and Dr. Myron Pollycove.

The work was performed under contract with the U.S. Atomic Energy Commission.

REFERENCES

1. Anger, Hal O.: Scintillation Camera with 11-Inch Image Detector. In Donner Laboratory Semiannual Report UCRL-11184, p. 69 (Fall 1963).
2. Anger, Hal O.: Gamma-Ray and Positron Scintillation Camera. *Nucleonics* 21: 10, 56, 1963.
3. Johansson, Sven A. E., and Skanse, Bengt: A Photographic Method of Determining the Distribution of Radioactive Material *in Vivo*. *Acta Radiologica* 39:317, 1953.
4. Kellershohn, C., and Pellerin, P.: Scintillator Grid Localizes Gamma Emitters Photographically. *Nucleonics* 13:12, 34, 1955.
5. Anger, Hal O.: Scintillation Camera. *Rev. Sci. Inst.* 29:27, 1958.
6. Anger, Hal O.: Radiation Image Device. U. S. Patent 3,011,057 (1961).
7. Bender, Merrill A., and Blau, Monte.: Autofluoroscopy: The Use of a Non-Scanning Device for Tumor Localization with Isotopes. *J. Nuclear Med.* 1:105, 1960.
8. Mallard, J. R., and Myers, M. J.: Clinical Applications of a Gamma Camera. *Phys. Med. Biol.* 8:183, 1963.
9. Bender, Merrill A., and Blau, Monte: The Autofluoroscope. *Nucleonics* 21:10, 52, 1963.
10. Anger, Hal O., and Davis, Donald H.: Gamma-Ray Detection Efficiency and Image Resolution of Sodium Iodide. *Rev. Sci. Inst.* 35:693, 1964.
11. Brucer, Marshall: Radioisotope Scanning. ORINS-20 (1958).
12. Brownell, G. L.: Theory of Radioisotope Scanning. *Int. J. Appl. Radiation and Isotopes* 3:181, 1958.
13. Francis, J. E., Bell, P. R., and Harris, C. C.: Medical Scintillation Spectrometry. *Nucleonics* 13:11, 82, 1955.
14. Mayneord, W. V.: Some Applications of Nuclear Physics to Medicine. *Brit. J. Radiol. Suppl.* 2:168, 1950.
15. Beck, R. N.: A Theoretical Evaluation of Brain Scanning Systems. *J. Nuclear Med.* 2:314, 1961.
16. Mather, R. L.: Gamma-Ray Collimator Penetration and Scattering Effects. *J. App. Phys.* 28:1200, 1957.
17. C. C. Harris, *et al*.: Collimators for Radioisotope Scanning, in *Progress in Medical Radioisotope Scanning,* p. 44, Oak Ridge Institute of Nuclear Studies, Oak Ridge, Tenn. (1962).
18. Anger, Hal O.: Scintillation Camera Image Recording. Lawrence Radiation Laboratory Report (UCRL-11336 (1964).
19. Harper, P. V., Becx, R., Charleston, D., and Lathrop, K. A.: Optimization of a Scanning Method Using Tc^{99m}. *Nucleonics* 22:Jan. 50, 1963.
20. Gottschalk, Alexander and Anger, Hal O.: Use of the Scintillation Camera to Reduce Radioisotope Scanning Time (*In Preparation*).